

# Multi-point Projection Phase TOF Ranging System

Xu Yuan and Lv Kang<sup>2 +</sup>

<sup>1</sup> Shenzhen Technology University, China

<sup>2</sup> Shenzhen Technology University, China

**Abstract.** TOF (Time of Flight) depth detection equipment is widely used in robotics, mobile phones, and medical fields. At present, flood light emission is the mainstream phase TOF light source emission scheme because of its relatively simple design and mature algorithm. However, in some application scenarios that do not require high resolution, the energy utilization rate of the light source part of the flood-type TOF system is low, which leads to a reduction in the measurement distance, and the dense optical path will aggravate the multi-path effect. For such scenarios, this paper proposes a multi-point projection scheme suitable for phase TOF. Compared with the floodlight scheme, this scheme has the following improvements: First, by adding a special optical diffraction device to the light source part of the module, the projected light spot can be distributed according to a specific light intensity, increasing the local light spot intensity and improving the energy utilization rate of the light source; The second is to propose an effective pixel selection scheme suitable for multi-point projection TOF to reduce depth map noise; The third is to provide a depth error correction method suitable for multi-point projection TOF, so that the accuracy can reach the millimeter level. Compared with the flood-phase TOF ranging solution with the same power consumption and volume, this solution can increase the ranging range by 2 times when the accuracy is the same; at the same distance, the power consumption is reduced by 3 times.

**Keywords:** time of flight, multi-point projection, phase TOF, photoelectric measurement.

## 1. Introduction

In recent years, the application of depth detection technology in the daily consumer market has become more and more extensive. At present, there are three mainstream depth detection technologies: binocular stereo vision [1-3], structured light [4-6] and TOF (time of flight) [7-9], among which structured light and TOF (time of flight) are due to their The active light source projection method has become the mainstream depth detection technology in the current consumer market. Compared with structured light technology, TOF technology requires less calculation and has better measurement stability in different distance scenarios. Therefore, the TOF (Time of Flight) solution is more favored by the consumer smart device market in medium and long distance and sports application scenarios. At present, the floodlight TOF scheme is the mainstream solution in the phase TOF technology system, because the floodlight projection can obtain a higher resolution depth map. However, for some application scenarios, such as sweepers, motion recognition, laser focusing and other scenarios, high resolution is not a necessary parameter, and dense beams will aggravate multi-path effects, resulting in large depth errors. Inspired by the structured light projection method [10-12], this paper proposes a multi-point projection phased TOF scheme. By improving the local spot intensity, increasing the maximum measurement distance, and reducing the power consumption of the module, the phase TOF can be more widely used in fields that do not require high resolution, such as cruise robots.

## 2. Structure and Composition

The multi-point projection TOF system can be divided into three major modules[13]: light modulation module, sampling module and calculation module, as shown in Fig. 1.

---

<sup>+</sup> Corresponding author. Tel.: + 13212798879;  
E-mail address: condysss@163.com.

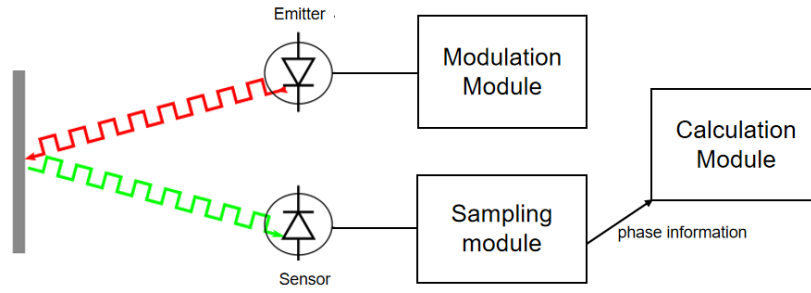


Fig. 1: System structure diagram

## 2.1. Modulation Module

The light source module of the multi-point projection phase TOF system is composed of a group of near-infrared VCSEL laser arrays, optical lenses and special optical diffraction devices, as shown in the left of Figure 2. The optical lens converges the light source of the laser array, and projects the converged light source into beams through the DOE[14], forming the effect on the right of Fig. 2.

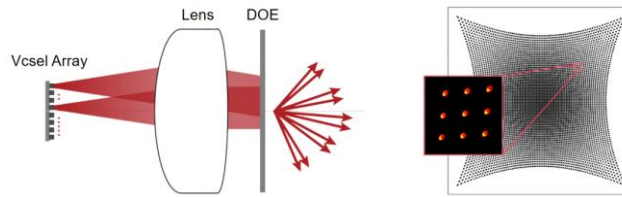


Fig. 2: Light source module diagram

## 2.2. Sampling Module

The multi-point projection phase TOF system uses a matrix sensor, and the simple structure diagram of each pixel on the sensor is shown in Figure 3.

The sampling block adjusts the opening and closing timing of switch 1 and switch 2 through the control unit, so that capacitor A and capacitor B collect optical signals with a phase difference of  $\pi$  positions, as shown in the right of Fig. 3, so that the differential charge of the two capacitors can eliminate the offset component make it directly related to the phase offset.

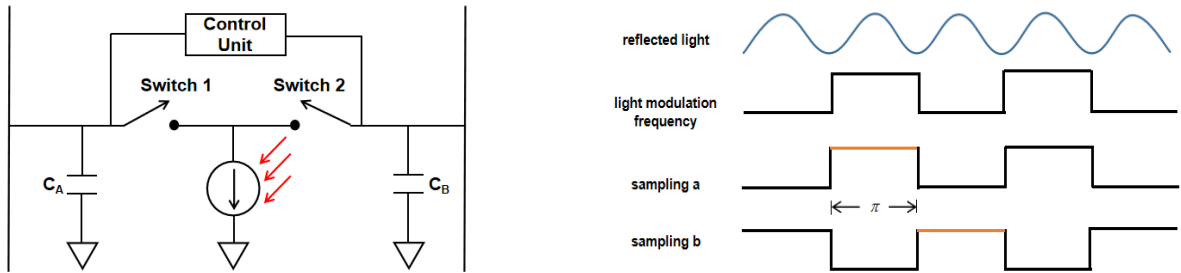


Fig. 3: Sampling module diagram

Therefore, the sampled signal can be established as a new mathematical formula, such as formula (1).

$$S = A \int_{\varphi_0}^{\varphi_0+\pi} \sin(\omega t - \Delta\varphi) d\omega t + B - (A \int_{\varphi_0+\pi}^{\varphi_0+2\pi} \sin(\omega t - \Delta\varphi) d\omega t + B) \quad (1)$$

$$= 4A * \cos(\omega t - \Delta\varphi)$$

In theory, the phase difference can be obtained by only sampling twice, but to improve accuracy, two sets of values are sampled more. Therefore, the new phase sample value can be expressed as:

$$S_1 = 4A * \cos(0 - \Delta\varphi) = 4A \cos \Delta\varphi \quad (2)$$

$$S_2 = 4A * \cos\left(\frac{\pi}{2} - \Delta\varphi\right) = 4A \sin \Delta\varphi \quad (3)$$

$$S_3 = 4A * \cos(\pi - \Delta\varphi) = -4A \cos \Delta\varphi \quad (4)$$

$$S_4 = 4A * \cos\left(\frac{3\pi}{2} - \Delta\varphi\right) = -4A \sin \Delta\varphi \quad (5)$$

### 2.3. Calculation Module

The calculation module of the multi-point projection phase TOF system includes two parts, the first part is the calculation of the original depth and amplitude; the second part is the depth correction calculation.

In Section 2.2, we obtained 4 sets of sampled values of the returned light. According to the model of the trigonometric cotangent function, the original phase shift can be calculated, as shown in equation (6).

$$\Delta\varphi = \arctan\left(\frac{\sin \Delta\varphi}{\cos \Delta\varphi}\right) = \arctan\left(\frac{S_1 - S_3}{S_2 - S_4}\right) \quad (6)$$

Combined with the light speed constant  $C$  and the light source modulation frequency, the original depth  $D$  and amplitude can be expressed as equations (7) and (8).

$$D = \frac{C * \Delta t}{2} = \frac{C * \Delta\varphi}{4\pi * f} \quad (7)$$

$$A_{\text{amp}} = 4A = \frac{\sqrt{(S_1 - S_3)^2 + (S_2 - S_4)^2}}{2} \quad (8)$$

Since the sensor of the multi-point projection system is a matrix, the depth of some pixels of the sensor is invalid, as shown in Fig. 4.

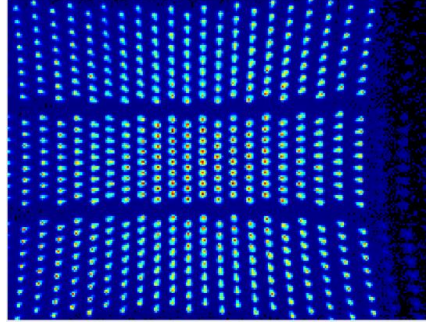


Fig. 4: Unprocessed magnitude map

As can be seen from Fig. 4, there is a lot of noise in the magnitude map, which not only affects the quality of the magnitude map, but also greatly reduces the quality of the depth map. Therefore, it needs to be filtered before outputting the depth map. First, use Gaussian filtering to remove obvious noise, then use the amplitude as the threshold to filter out the pixels below the threshold to form a lattice local spot, and finally use the maximum filter to select the pixels in the local spot, and select the representative point of the spot, the specific process is shown in Fig. 5.

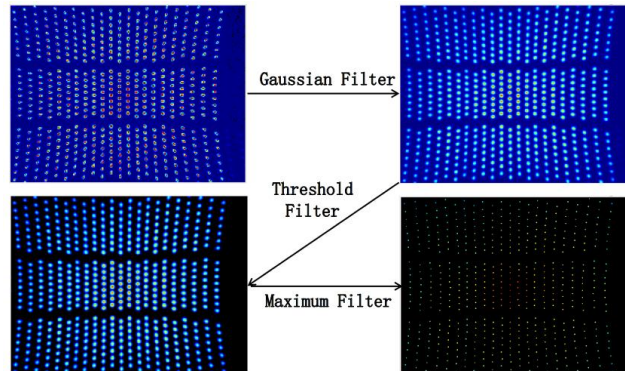


Fig. 5: Filter processing

The multi-point projection phase TOF system is affected by the temperature error and the wobble error like the traditional phase TOF system, so it is necessary to perform depth correction on the original depth of the representative pixel point.

The influence of temperature on semiconductor systems[13] has been proven many years ago, and in multi-point projection phase TOF systems, the pixel measurement depth increases linearly with the increase of temperature, so we need to calibrate temperature coefficient  $T$  of the module before working. The calibration method is very simple. Just fix the module in the incubator, and then linearly increase the temperature of the incubator. During this process, collect the discrete values of the temperature and depth values of the module and obtain the temperature coefficient  $T$  through these discrete values. In the subsequent measurement work, the temperature habit coefficient  $T$  can be used to correct the temperature error in the measurement process in real time by equation (9). Where  $S_{cor}$  represents the corrected depth,  $S$  represents the depth containing the temperature error, and  $TEM_{cur}$  represents the current TOF module temperature.

$$S_{T_{cor}} = S + T * TEM_{cur} \quad (9)$$

Wobble error is a common error in phase-based TOF systems, mainly due to non-ideal modulation and demodulation of the light source and sensor. The error form is shown in Fig. 6.

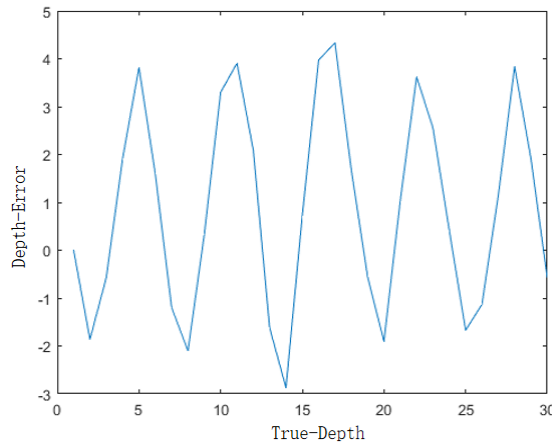


Fig. 6: Wobble error diagram

For the wobble error, the phase TOF system usually uses the interpolation look-up table method to correct it, and collects a set of discrete values  $(d_1, d_2, d_3 \dots d_i)$  covering the entire measurement range through the method of internal delay at the same interval, and through the least squares method, a linear fitting is performed on these discrete values, and the first-order coefficient is obtained. Finally, the correction of the wobble error is completed through the equation (10).  $S$  represents the depth to be corrected, and  $S_{cor}$  represents the depth after correction in the equation (10).

$$S_{cor} = \frac{S - d_i}{d_{i+1} - d_i} \cdot K + d_i \quad (d_i < s < d_{i+1}) \quad (10)$$

The multi-point projection phase TOF system has another problem with the wobble error. Since the projected light spot is a discrete dot matrix, during the wobble error calibration, not every pixel of the sensor has a calibration table, and due to the parallax effect, when the measurement depth changes, the position of the effective point on the sensor will also change, when the effective point moves to a pixel point without a calibration table, the wobble error of this point cannot be corrected. In view of this situation, we place the diffuser on the lamp bead in parallel to re-generalize the dot matrix light spot, so that each pixel on the sensor can obtain the calibration table during calibration. The effect of placing the diffuser is shown in the fig. 7.

Since the maximum measurement distance of the multi-point projection phase TOF system is limited by the modulation frequency, when the phase difference corresponding to the measurement distance exceeds  $\pi$ , the phase blur phenomenon will occur, that is, the number of cycles at this time cannot be determined.

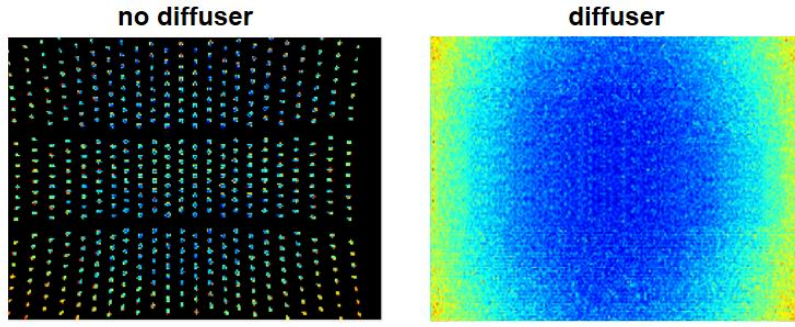


Fig. 7: Place the diffuser

Although low-frequency modulation can be used to increase the maximum measurement range, it will lose measurement accuracy. In order to ensure high precision and increase the maximum measurement distance, we use the dual-frequency positioning method to determine the specific position of the current phase difference. The specific steps are as follows:

Assuming that the modulation frequencies of the modules are  $f_1$  and  $f_2$ , respectively, the integer ratios  $N_1$  and  $N_2$  of  $f_1$  and  $f_2$  that are mutually prime can be calculated. Using the characteristics of frequency conversion and constant distance, the formula (11) can be derived, where  $n_1 < N_1 - 1$ ,  $n_2 < N_2 - 1$ ,  $\varphi_1$ ,  $\varphi_2$  and represent the phases measured by the dual frequency of the module respectively. According to the characteristic that  $n_1$  and  $n_2$  are positive integers in Equation (11), solve Equation (12) to get the values of the cycle numbers  $n_1$  and  $n_2$ , and finally substitute them into Equation (13) to get the exact phase difference value. Use high-frequency phase calculations to ensure measurement accuracy.

$$n_1 \cdot 2\pi + \varphi_1 = n_2 \cdot 2\pi + \varphi_2 \quad (11)$$

$$\min |(n_1 \cdot 2\pi + \varphi_1) - (n_2 \cdot 2\pi + \varphi_2)| \quad (12)$$

$$\Delta\varphi = n_1 \cdot 2\pi + \varphi_1 = n_2 \cdot 2\pi + \varphi_2 \quad (13)$$

### 3. Experiment Procedure

#### 3.1. Experimental Platform

The experimental platform is the NV08 area-array TOF camera of Nephotonics Technology. The NV08 includes a flood-type projection light source, a depth sensor, a power supply module, an RJ-45 network port module and the corresponding drive circuit, as shown in Fig 8.



Fig. 8: NV08 area scan TOF camera



Fig. 9: Installation of the point projection module

We use the point projection module of multi-point projection to replace the original flood projection light source module of the platform, as shown in Fig. 9. After the replacement is completed, the power supply test is performed on the module, and the four-phase sampling value of each pixel is obtained through the network interface, and then the amplitude value of each pixel is obtained and visualized using the matrix operation of MATLAB. The schematic diagram of the effect is shown in Fig. 10.

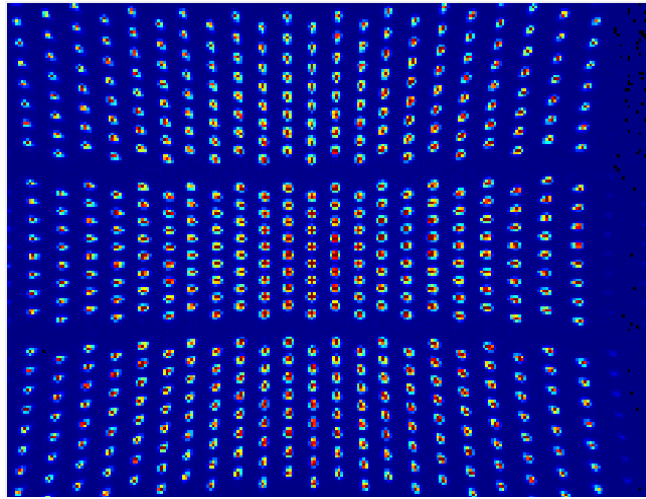


Fig. 10: Multi-point projection renderings

After the module successfully outputs the depth, we sequentially calibrate the temperature of the module and calibrate the swing error table of the installed flood plate. The calibration process is as follows:

### 3.2. Calibration Process

1. Temperature coefficient calibration:

- a) Fix the module in the incubator and connect it to the network.
- b) Adjust the temperature of the incubator, the adjustment range is 10 °C to 70 °C, and the interval is 5 °C.
- c) Obtain and record the temperature data of each interval point of the temperature sensor through the corresponding SDK.

2. Wobble error table calibration:

- a) Power on the module and fix it at a distance of 100cm from the calibration plane.
- b) Adjust the internal delay interval, the number of intervals is 24.
- c) Collect the depth value of each pixel point in each time interval, that is, the wobble error table value.

### 3.3. Maintaining the Integrity of the Specifications

After completing the above two calibrations, the performance test comparison between the multi-point projection phase TOF system and the traditional flood phase TOF system is started. The test process is as follows.

- a) Power on the module and fix it at a distance of 20cm from the test plane, and enable automatic integration to ensure that the two modules can exert maximum performance.
- b) After the integration time is stable, the depth value of each pixel is collected and averaged.
- c) Move the module 20cm away from the test plane and repeat step 2.
- d) Repeat step 3 until the distance between the module and the test plane is 400cm.

## 4. Result Analysis

The performance test results are mainly analyzed from three aspects: test distance, amplitude value and integration time(sampling time). The test results are shown in Fig. 11.

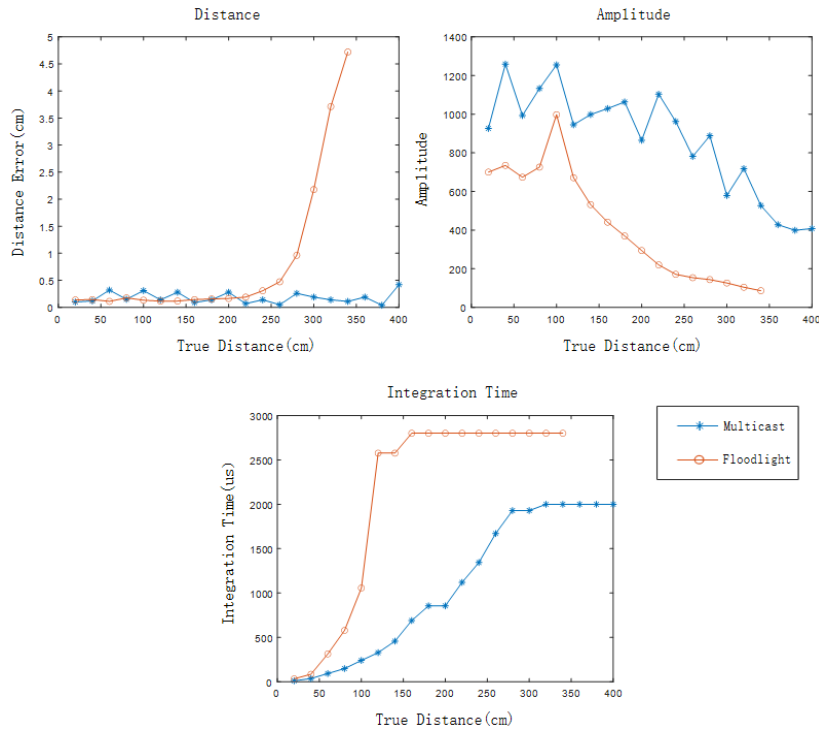


Fig. 11: Comparison of multi-point projection and floodlight effects

From the comparison chart, it can be seen that the depth error of the flood-type TOF module is stable within 0.5cm before the measurement distance of 280cm, and the minimum amplitude value at this time is about 170. When it exceeds 280cm, the amplitude value gradually decreases, and the depth error increases rapidly as the measurement distance increases. This is caused by the distance is too far and the return light intensity is not enough. And the measurement distance is about 180cm, the integration time reaches the maximum value, which means that the module function consumption reached the maximum value. In contrast, the multi-point projection module still has an amplitude value of about 400 when the measurement distance is 400cm, the error of the full depth value is also stable within 0.4cm, and the integration time reaches the maximum value when the measurement distance is 330cm. Therefore, the test results show that under the same light source power, the multi-point projection TOF module not only has a longer measurement distance than the flood-type TOF module, but also has a smaller error in the measurement depth value at a long distance. When the distance is longer, the integration time is shorter and the power consumption is lower. And it can be seen from Table 1 that, compared with other 3D imaging technologies, although the measurement accuracy of TOF at close range is not as good as that of structured light and binocular vision, in the measurement range, the influence of outdoor work on the module and the imaging frame rate three There are obvious advantages.

Table 1: Depth Detection Technology Comparison

	TOF	Binocular Vision	Structured Light
Ranging method	<b>Active</b>	Passive	<b>Active</b>
Measurement Accuracy	<1cm	<b>&lt;1mm</b>	<b>&lt;1mm</b>
Measuring Range	<b>&lt;10m</b>	<1m	<80cm
Outdoor Work Impact	<b>Little</b>	Middle	Middle
Frame Rate	<b>100</b>	30-100	30

## 5. Conclusion

Through the comparative test results in the fourth section, it can be proved that the multi-point projection phase TOF system is superior to the traditional flood phase TOF system in both measurement distance and

power consumption. But this is because the former sacrifices the resolution of the depth map, but for application scenarios such as sweeping robots or cargo robots that do not require high resolution, multi-point projection is more advantageous. In response to the reduction of resolution, multiple depth images can be acquired according to the rotation module and the density of the depth point cloud image can be improved through multi-image fusion technology, so as to restore the characteristics of the measured object as much as possible.

## 6. Acknowledgements

This article is supported by Shenzhen Technology University of School-Enterprise Cooperation Foundation.

## 7. References

- [1] Sun X , Jiang Y , Ji Y , et al. Distance Measurement System Based on Binocular Stereo Vision[J]. IOP Conference Series Earth and Environmental Science, 2019, 252(5):052051.
- [2] Lea, Steffen, Daniel, et al. Neuromorphic Stereo Vision: A Survey of Bio-Inspired Sensors and Algorithms.[J]. Frontiers in neurorobotics, 2019, 13:28-28.
- [3] Fan R, Wang L, Bocus M J, et al. Computer Stereo Vision for Autonomous Driving[J]. arXiv, 2020.
- [4] Salvi J, Pages J, Batlle J. Pattern codification strategies in structured light systems[J]. Pattern recognition, 2004, 37(4): 827-849.
- [5] Wei, Yin, Shijie, et al. High-speed 3D shape measurement using the optimized composite fringe patterns and stereo-assisted structured light system[J]. Optics Express, 2019, 27(3):2411-2431.
- [6] Zhong F, Kumar R, Quan C. A cost-effective single-shot structured light system for 3D shape measurement[J]. IEEE Sensors Journal, 2019, 19(17): 7335-7346.
- [7] Bulczak D , Lambers M , Kolb A . Quantified, Interactive Simulation of AMCW ToF Camera Including Multipath Effects[J]. Sensors, 2018, 18(2):13-13.
- [8] Liu J, Sun Q, Fan Z, et al. TOF lidar development in autonomous vehicle. 2018 IEEE 3rd Optoelectronics Global Conference (OGC) [C]. Shenzhen(CN). 2018. IEEE, 2018: 185-190.
- [9] Anthonys G. ToF Range Imaging Cameras[M]. Timing Jitter in Time-of-Flight Range Imaging Cameras. Springer, Cham, 2022: 19-37.
- [10] Jia T, Wang B N, Zhou Z X, et al. Scene depth perception based on omnidirectional structured light[J]. IEEE Transactions on image processing, 2016, 25(9): 4369-4378.
- [11] Duda A, Schwendner J, Gaudig C. SRSL: Monocular self-referenced line structured light[C]//2015 IEEE/RSJ International Conference on Intelligent Robots and Systems (IROS). IEEE, 2015: 717-722.
- [12] Kuan Y W, Ee N O, Wei L S. Comparative study of intel R200, Kinect v2, and primesense RGB-D sensors performance outdoors[J]. IEEE Sensors Journal, 2019, 19(19): 8741-8750.
- [13] Foix S, Alenya G, Torras C. Lock-in time-of-flight (ToF) cameras: A survey[J]. IEEE Sensors Journal, 2011, 11(9): 1917-1926.
- [14] Tong Z, Sun C, Ma Y, et al. Design and implementation of passive speckle reduction in laser projector with refractive optical element and lenslet integrator[J]. Optik, 2022, 252: 168531.